

Efficient Multi-Carrier Communication over Mobile Wideband Channels

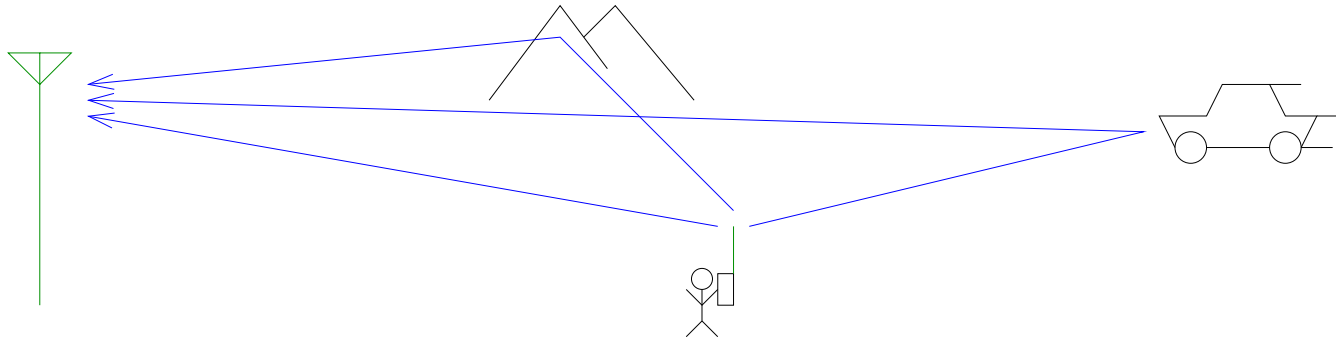
Phil Schniter



July 2008

(Joint work with Mr. Sungjun Hwang and Dr. Sib Das)

Multipath, Mobility, and Bandwidth:



Trends:

- As the signal bandwidth increases, there are more gain variations across the signal bandwidth, and hence more channel parameters.

Increased BW \Rightarrow longer channel impulse response.

- As the mobilities of the transmitter, receiver, and reflectors increase, there are more channel gain variations per unit time.

Increased mobility \Rightarrow faster impulse response variation.

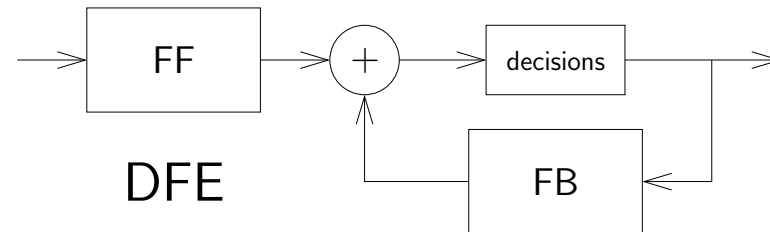
Multipath Fading (cont.):

- Implication:

As bandwidth & mobility increase, time-domain receivers need to implement longer filters and adapt them at faster rates.

- Example — North American Digital TV:

Typical receivers use decision feedback equalization (DFE) with 1000 taps in the feedforward path and 500 in the feedback path.

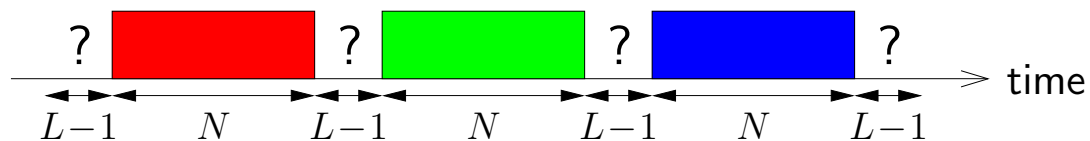


Even with a fixed transmitter and receiver, it is very difficult to adapt such long filters quickly enough!

Orthogonal Frequency Division Multiplexing (OFDM):


Main Ideas:

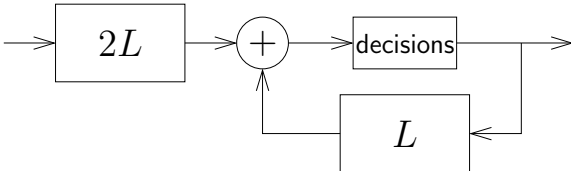
1. *Transmit data in parallel over non-interfering narrowband subchannels.*
 - Flat frequency response across each subchannel $\Rightarrow 1 \frac{\text{channel coefficient}}{\text{subchannel}}$.
 - Equalization = one complex gain adjustment per subchannel!
2. *Implement subchannelization using the Fast Fourier Transform (FFT).*
 - No calibration or drift issues like with analog modulators.
 - Minimal frequency spacing (\Rightarrow good spectral efficiency).
 - Fast implementation: $N \log_2 N$ multiplications per N -FFT.
 - Requires a guard interval of length- $L-1$.

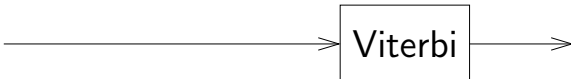


Equalization Complexity:

Single-carrier:

Linear:  $3L$ mults per QAM symbol

DFE:  $3L$ mults per QAM symbol

MLSD:  $|\mathcal{S}|^L$ mults per QAM symbol

Complexity scales *linearly* or *exponentially* in the channel length L .

Multi carrier:

$N + N \log_2 N$ mults per block, where typically $N \approx 4L$.

$\Rightarrow 1 + \log_2 N = \boxed{3 + \log_2 L}$ mults per QAM symbol.

Complexity scales *logarithmically* in the channel length L .

Example: When $L = 512$, we have $3L = 1536$ and $3 + \log_2 L = 12$.

CP-OFDM:

Principal advantage:

- Low-complexity demod with delay-spreading (i.e., freq selective) chans.

Some disadvantages:

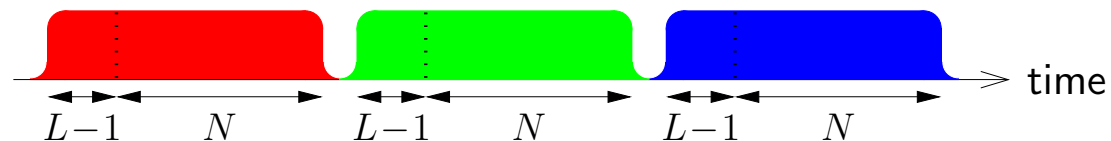
- Sensitive to Doppler-spreading (i.e., time selective) channels.
- Loss of spectral efficiency due to the insertion of guards.

What if we increased N relative to L (i.e., $P \triangleq \frac{N}{L} \gg 4$)?

- Complexity increases to $1 + \log_2 P + \log_2 L$ $\frac{\text{mults}}{\text{QAM symbol}}$...not bad.
- Reduced subcarrier spacing \Rightarrow more sensitive to Doppler spread!

- Slow spectral roll-off causes interference to adjacent-band systems.

Improves with raised-cosine pulse, but at further loss in efficiency:



- High peak-to-average power ratio (PAPR).

The Big Question:

Can we fix CP-OFDM's

- *sensitivity to Doppler spread*
- *loss in spectral efficiency, and*
- *slow spectral roll-off,*

without spoiling its $\mathcal{O}(\log_2 L)$ $\frac{\text{mults}}{\text{QAM symbol}}$ complexity scaling?

The Big Question:

Can we fix CP-OFDM's

- *sensitivity to Doppler spread*
- *loss in spectral efficiency, and*
- *slow spectral roll-off,*

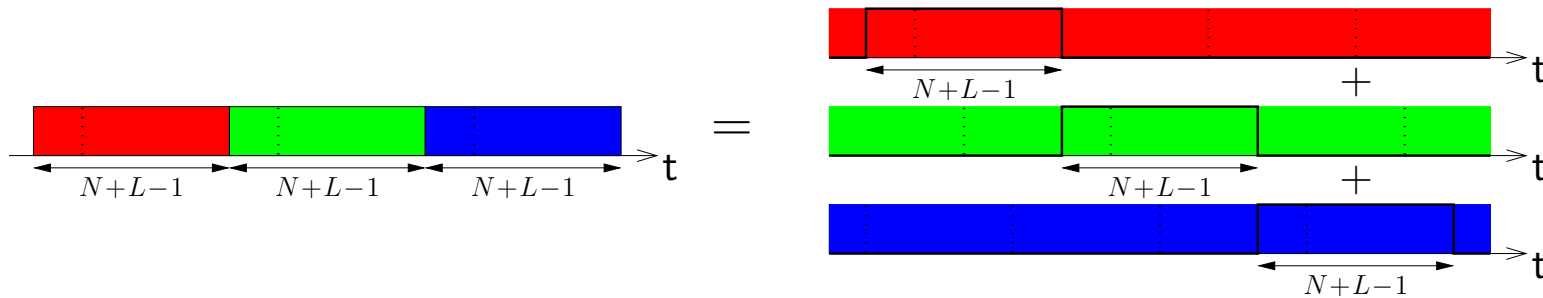
without spoiling its $\mathcal{O}(\log_2 L)$ $\frac{\text{mults}}{\text{QAM symbol}}$ complexity scaling?

Yes!

Re-think the role of “pulse shaping” in multi-carrier modulation...

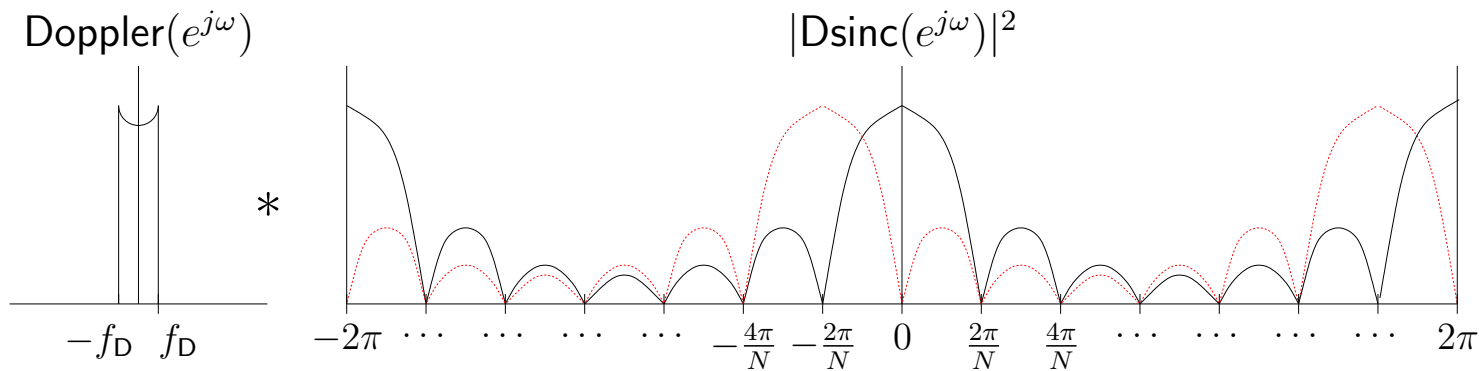
Rectangular Pulses:

A standard CP-OFDM block can be recognized as a sum of N infinite-length complex exponentials windowed by a rectangular pulse of width $N+L-1$.



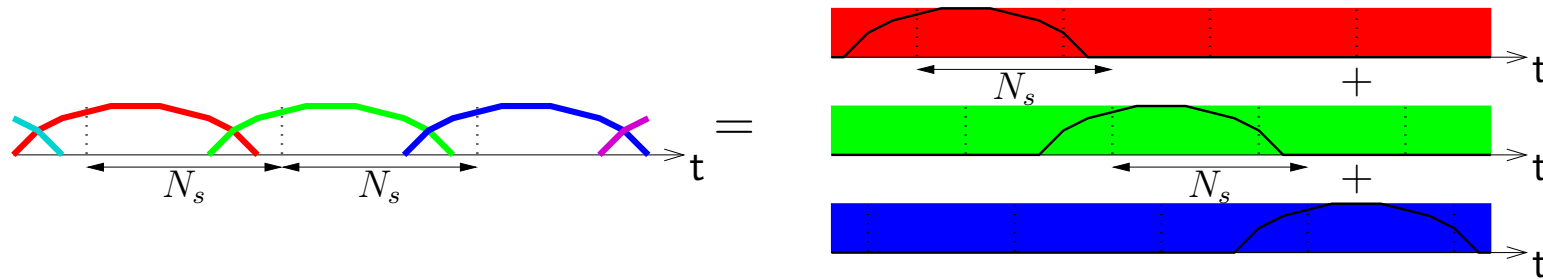
⇒ *Dirichlet sinc* in DTFT domain, whose slow side-lobe decay causes:

- strong interference to adjacent-band communication systems, and
- high sensitivity to Doppler spreading:



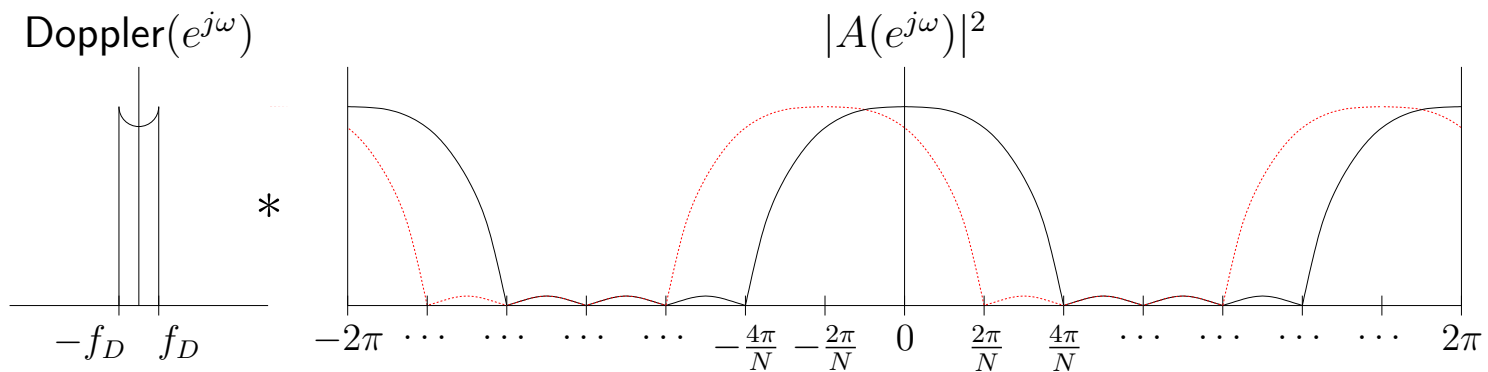
Smooth Overlapping Pulses:

What if we applied a *smooth* window instead?



The main-lobe is *wider* but the sidelobes *decay more quickly*, implying:

- reduced adjacent-band interference, and
- strong interference from adjacent subcarriers, but very little interference from all other subcarriers, even under large Doppler spreads:



Smooth Overlapping Pulses:

Challenge: The use of smooth overlapping pulses potentially causes *inter-carrier interference* (ICI) and *inter-block interference* (IBI):

$$\mathbf{x}(i) = \sum_{q=-\infty}^{\infty} \underbrace{\mathbf{H}(i, q)}_{\substack{\text{subcarrier} \\ \text{coupling matrix}}} \mathbf{s}(i - q) + \mathbf{z}(i). \quad \text{Difficult to equalize!}$$

Solution: Design the pulse shapes with the goal of...

1. Completely suppressing IBI: $\mathbf{H}(i, q)|_{q \neq 0} = \mathbf{0}$.
2. Allowing ICI only within a radius of $D \ll N$ subcarriers. (Often $D = 1$.)

$$\mathbf{x}(i) = \mathbf{H}(i, 0) \mathbf{s}(i) + \mathbf{z}(i)$$

Not difficult to equalize.

Receiver Pulse-Shaping:

Though so far we've considered a non-rectangular *transmission pulse* $\{a_n\}$,

$$t_n = \sum_{i=-\infty}^{\infty} a_{n-iN_s} \sum_{k=0}^{N-1} s_k(i) e^{j\frac{2\pi}{N}kn}, \quad n = -\infty \dots \infty,$$

we can use, in addition, a non-rectangular *reception pulse* $\{b_n\}$:

$$x_k(i) = \sum_{n=-\infty}^{\infty} r_{n-iN_s} b_n e^{-j\frac{2\pi}{N}kn}, \quad k = 0 \dots N-1.$$

N_s specifies the interval between the start of one OFDM block and the next.

- Modulation efficiency $\eta \triangleq \frac{N \text{ symbols}}{N_s \text{ sec Hz}}$
- For OFDM, $N_s = N + L - 1$, but now there is *no constraint* on N_s !

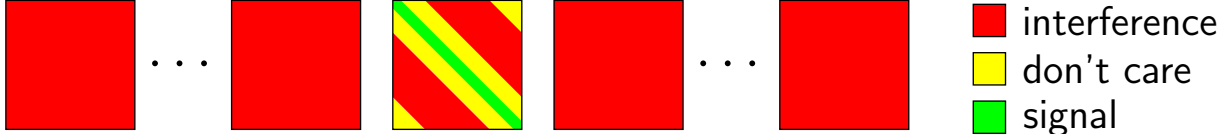
We focus on $N_s = N \Leftrightarrow$ *no guard interval* $\Leftrightarrow \eta = 1$.

Max-SINR Pulse Design:

Writing the received signal energy components due to

$$\mathcal{E}_s = \sum_{(q,k,l) \in \blacksquare} \mathbb{E}\{|H_{k,l}(\cdot, q)|^2\} \quad \text{“signal” and}$$

$$\mathcal{E}_i = \sum_{(q,k,l) \in \blacksquare} \mathbb{E}\{|H_{k,l}(\cdot, q)|^2\} \quad \text{“interference” (IBI+ICI)}$$

where $\{\mathbf{H}(\cdot, q)\} =$ 

we can write

$$\text{SINR} = \frac{\mathcal{E}_s}{\mathcal{E}_i + \mathcal{E}_n} = \frac{\mathbf{a}^H \mathbf{P}_1(\mathbf{b}) \mathbf{a}}{\mathbf{a}^H \mathbf{P}_2(\mathbf{b}) \mathbf{a}} = \frac{\mathbf{b}^H \mathbf{P}_3(\mathbf{a}) \mathbf{b}}{\mathbf{b}^H \mathbf{P}_4(\mathbf{a}) \mathbf{b}}$$

where

\mathbf{a} = transmission pulse coefficients

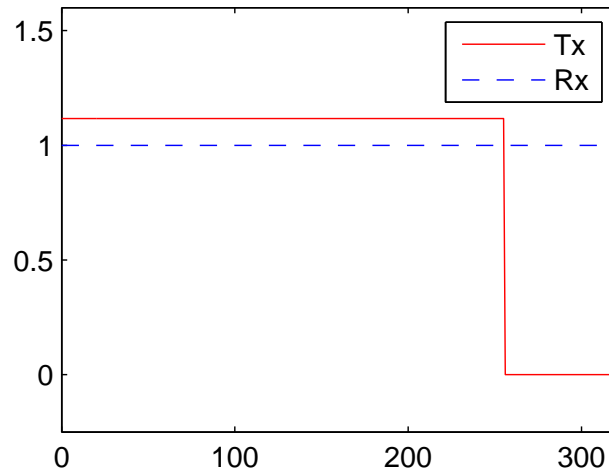
\mathbf{b} = reception pulse coefficients

$\mathbf{P}_1(\cdot), \mathbf{P}_2(\cdot), \mathbf{P}_3(\cdot), \mathbf{P}_4(\cdot)$ = matrix fxns dependant on Doppler & SNR.

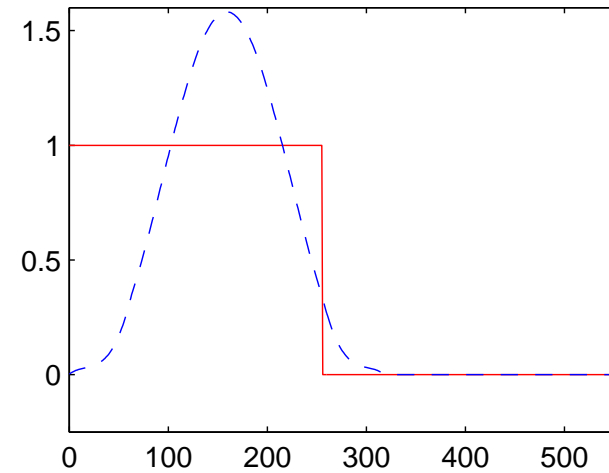
\Rightarrow SINR-maximizing pulses are generalized eigenvectors.

Max-SINR Pulse Examples:

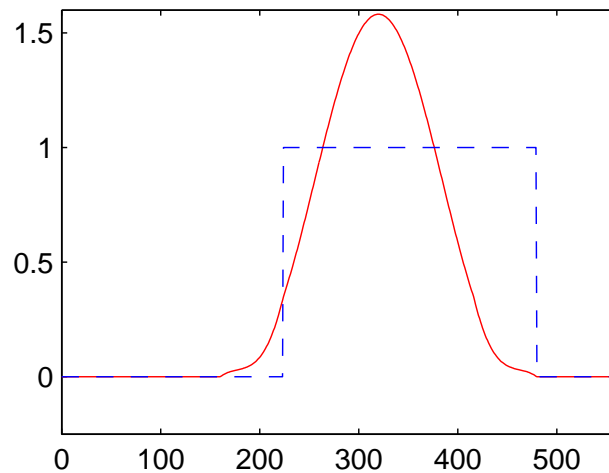
ZP-OFDM ($\eta = 0.803$)



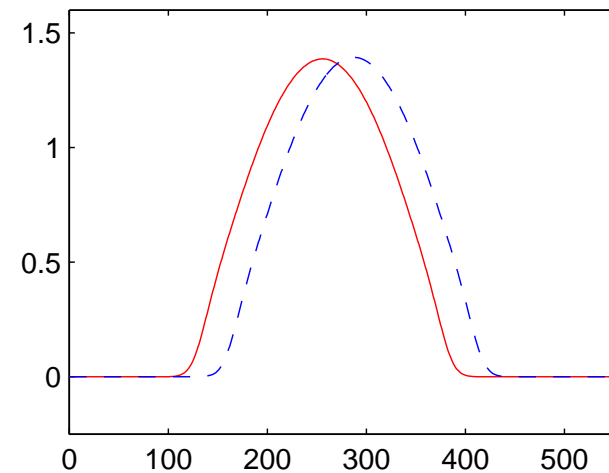
Optimized receiver ($\eta = 1$)



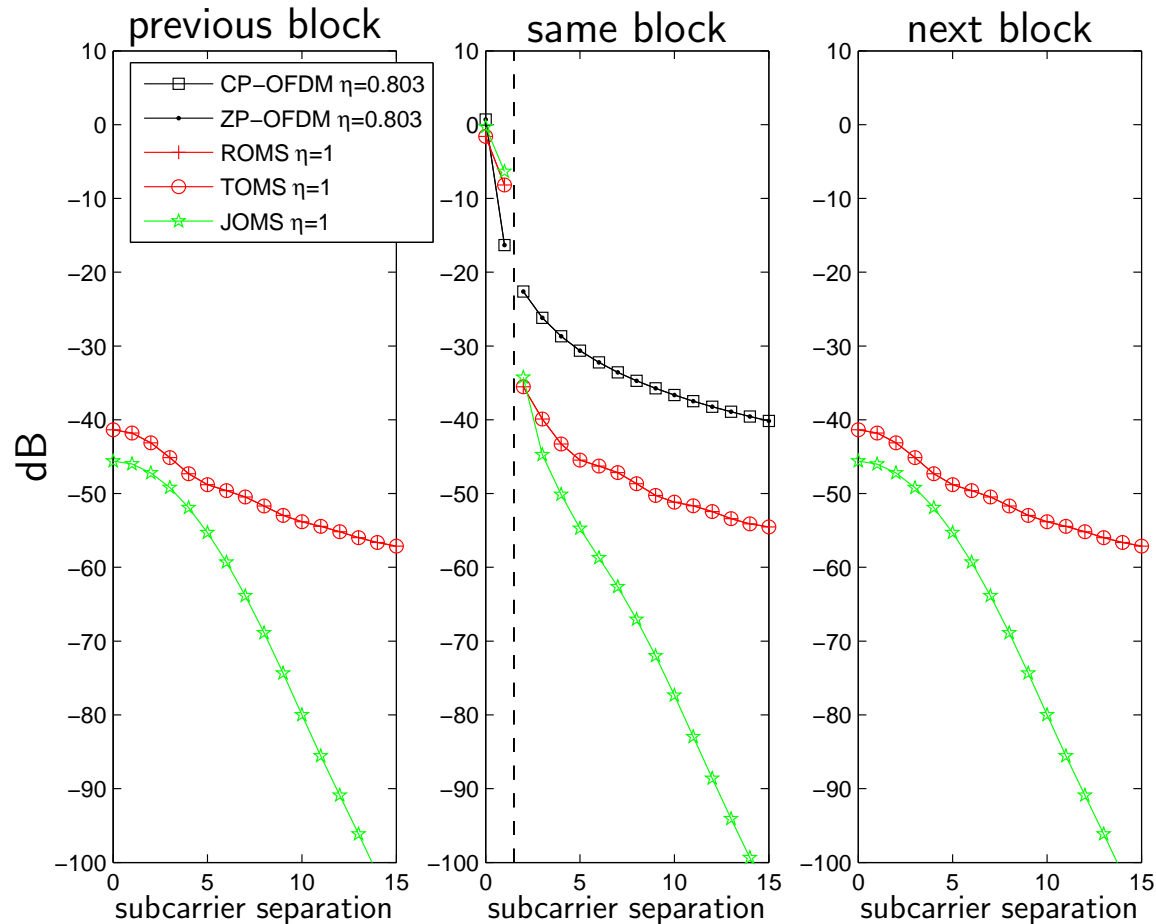
Optimized transmitter ($\eta = 1$)



Jointly optimized ($\eta = 1$)



IBI/ICI Energy Profiles (same for each subcarrier):



$D = 1$, $\text{SNR} = 15\text{dB}$, $L = 64$, $f_D T_c = 7.6 \times 10^{-4}$, Jakes Doppler spectrum.
 (For example, $f_c = 20\text{GHz}$, $\text{BW} = 3\text{MHz}$, $T_h = 5.4\mu\text{s}$, $v = 120\text{km/hr.}$)

Non-Orthogonal FDM:

To summarize, Orthogonal FDM is possible only when

1. the channel is time-invariant, and
2. an adequate-length guard is included.

With a properly-designed *Non-Orthogonal FDM*, we can

- eliminate the guard, and
- tolerate large delay and Doppler spreads,

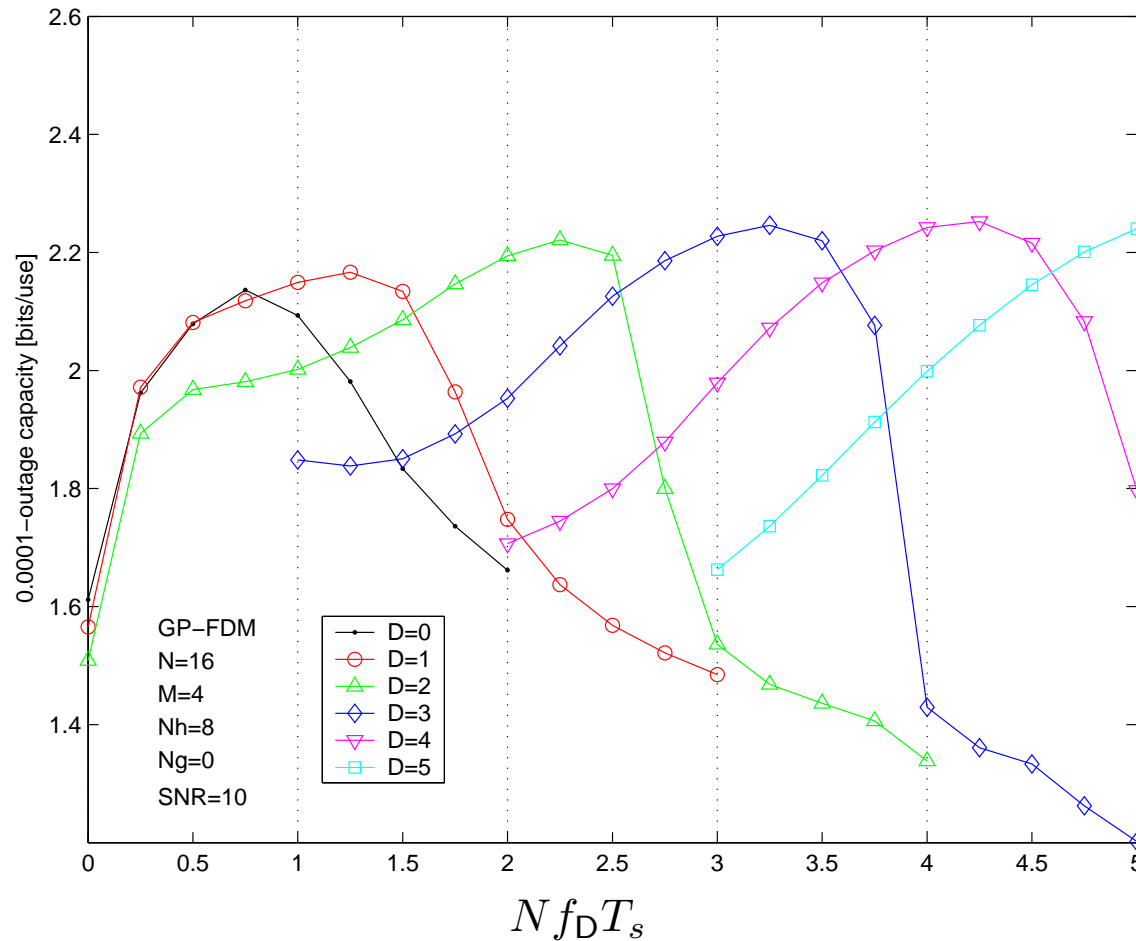
at the cost of

- a short span of intercarrier-interference,

which can be properly handled via low-complexity equalization.

Thus, we advocate *shaping ISI/ICI* rather than *suppressing ISI/ICI*.

Outage Capacity vs $Nf_D T_s$ for various ICI-radii D :



- The outage-capacity optimal D obeys $D \approx \lfloor Nf_D T_s \rfloor$!
- ICI shaping is better than ICI suppression when $2f_D T_s \geq \frac{1}{N}$.

ICI Equalization:

Coherent approaches (i.e., known channel):

- | | $\frac{\text{mults}}{\text{QAM symbol}}$ |
|--|--|
| 1. Viterbi [Matheus/Kammeyer GLOBE 97] | $\mathcal{O}(\mathcal{S} ^D D)$ |
| 2. Iterative Soft [Das/Schniter Asilomar 04] | $\mathcal{O}(D^2)$ |
| 3. Linear MMSE [Rugini/Banelli/Leus SPL 05] | $\mathcal{O}(D^2)$ |
| 4. MMSE DFE [Rugini/Banelli/Leus SPAWC 05] | $\mathcal{O}(D^2)$ |
| 5. Tree Search [Hwang/Schniter SPAWC 06] | $\mathcal{O}(D^2)$ |

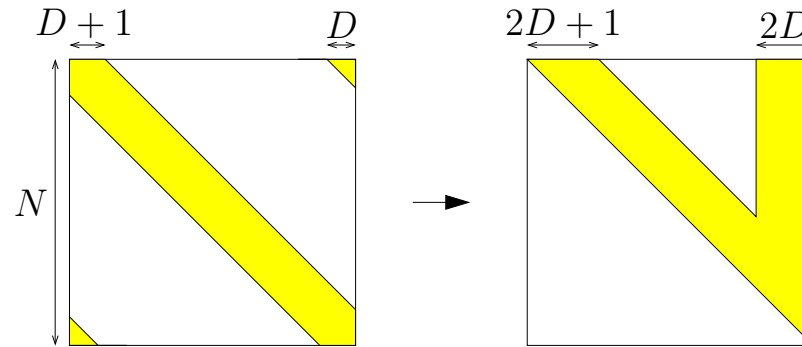
Non-coherent approaches (i.e., unknown channel):

- | | |
|--|------------------------|
| 1. Hard Tree Search [Hwang/Schniter WUWNet 07] | $\mathcal{O}(D^2 L^2)$ |
| 2. Soft Tree Search [Hwang/Schniter Asilomar 07] | $\mathcal{O}(D^2 L^2)$ |

1) Coherent Tree Search:

Two-step procedure:

1. MMSE-GDFE pre-processing [Damen/ElGamal/Caire TIT 03]:

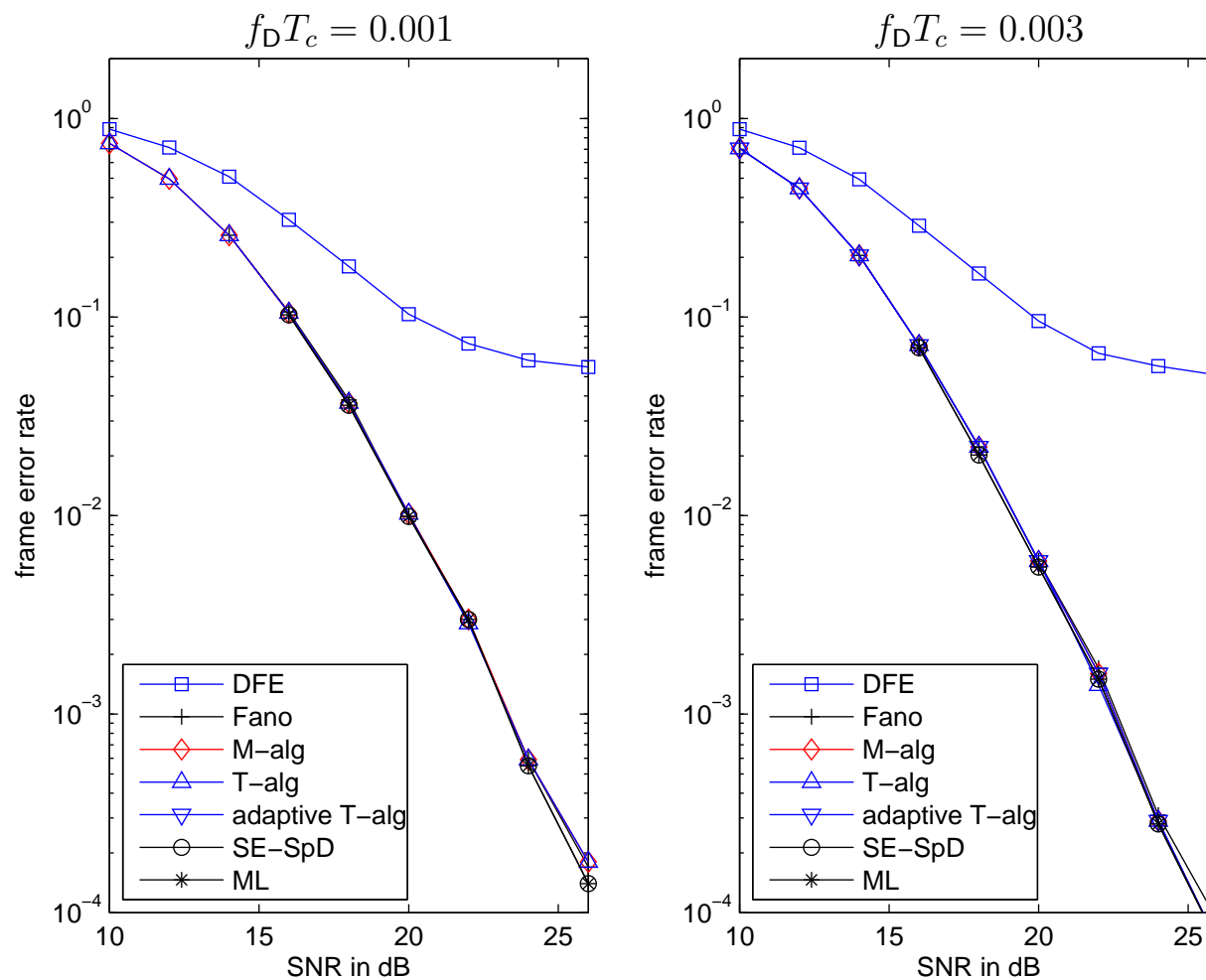


$\rightsquigarrow \mathcal{O}(D^2N)$ algorithm [Rugini/Banelli/Leus SPAWC 05].

2. Near-optimal yet efficient tree search. Options include:

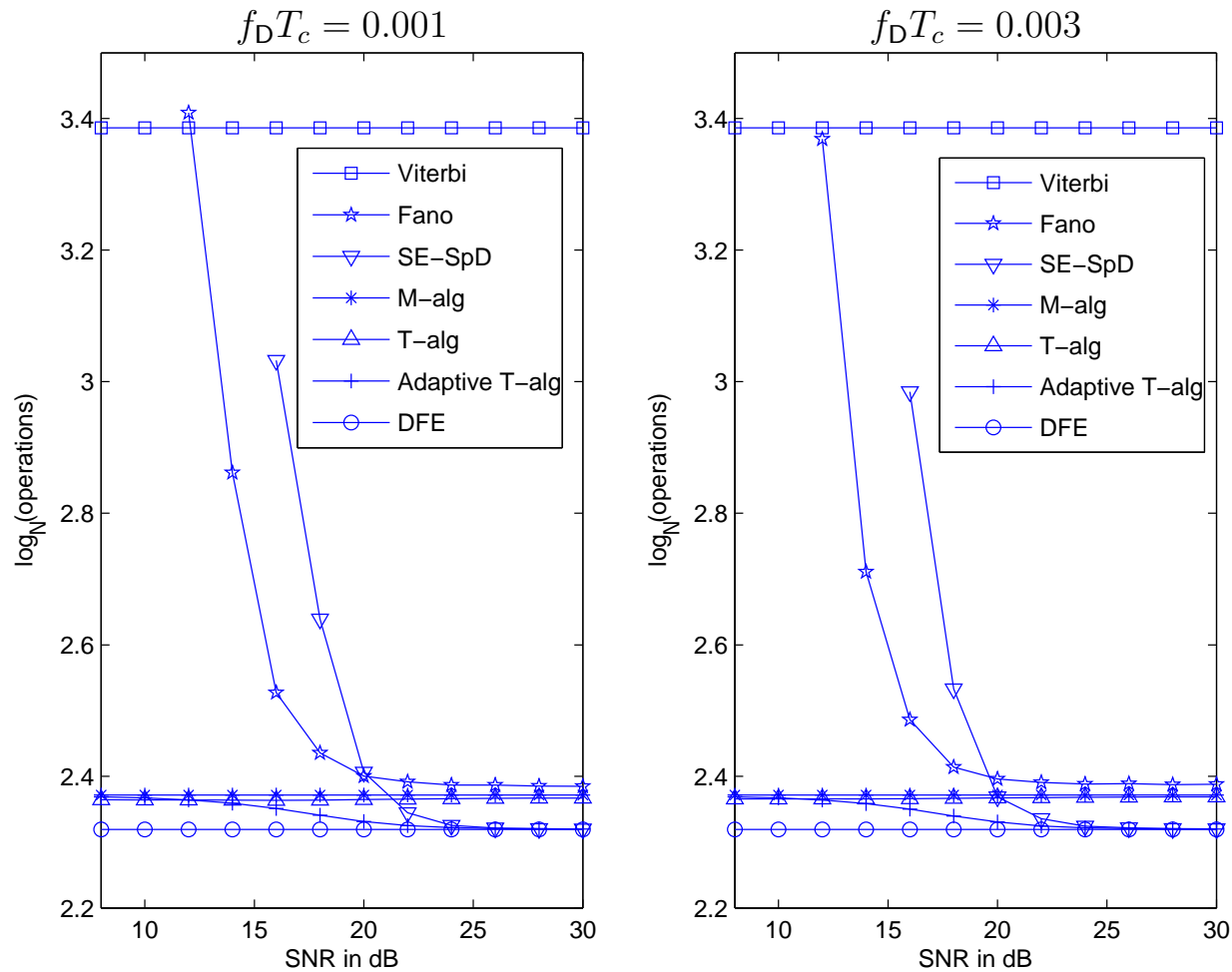
- Depth-first search (e.g., Schnor-Euchner sphere decoder),
- Best-first search (e.g., Fano alg, stack alg),
- Breadth-first search (e.g., M-alg, T-alg, Pohst sphere decoder).

Performance:



Suboptimal tree search is almost indistinguishable from ML!

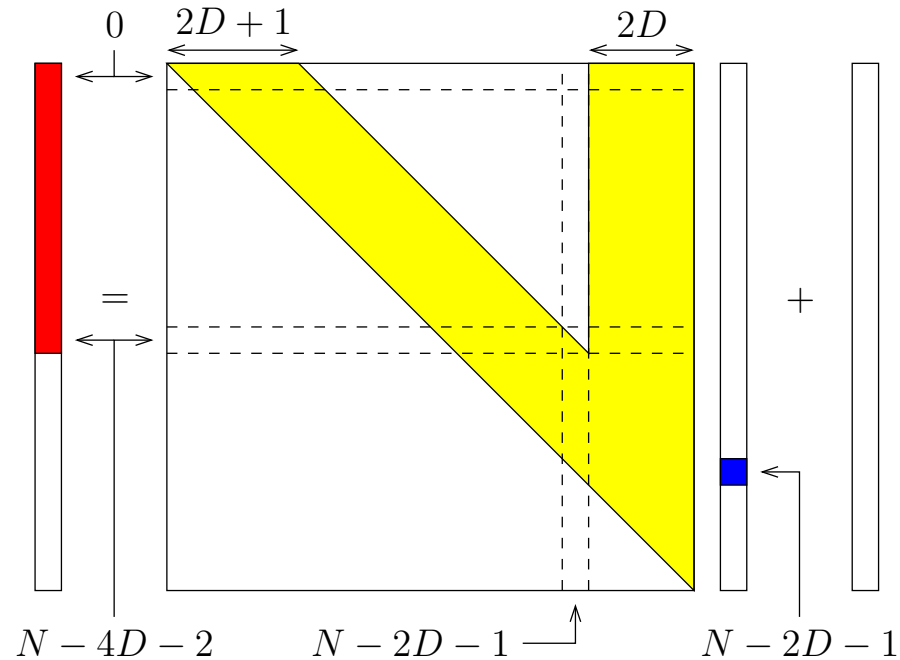
Average Complexity (MACs/frame):



Breadth-first & DFE stay cheap, while depth-first & Fano explode!

Error Masking due to V-shaped Channel Matrix:

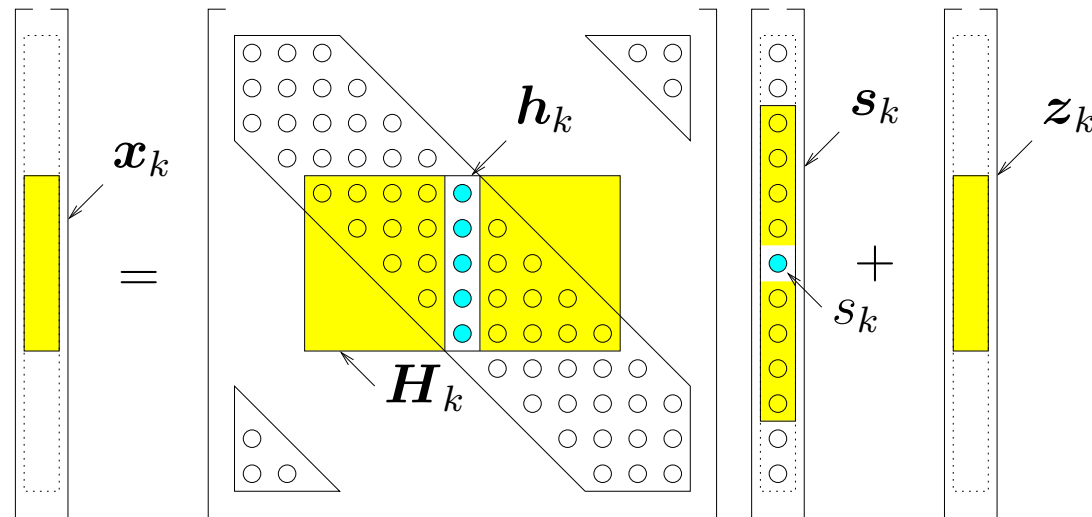
After MMSE-GDFE pre-processing, we get the following system:



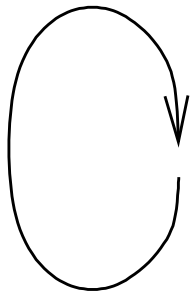
Key point: The **blue** symbol does not affect any of the **red** observations.

Error-masking explains the complexity explosion of the depth-first and Fano searches!

2) Iterative Soft ICI Cancellation:

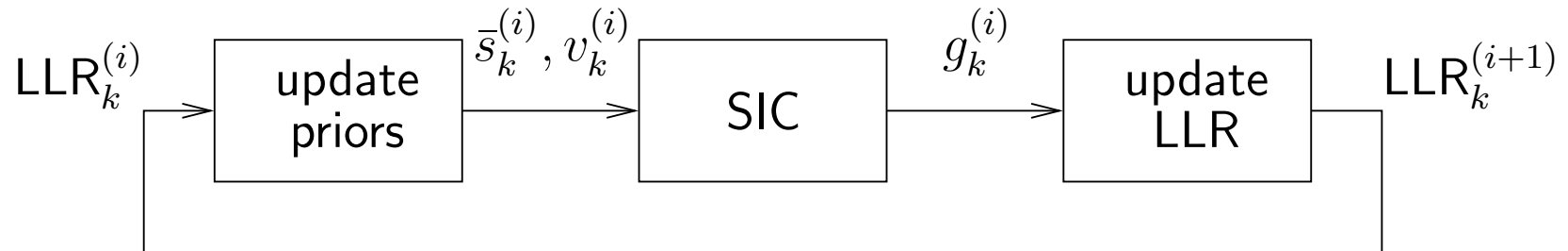


$$\mathbf{x}_k = \mathbf{H}_k \mathbf{s}_k + \mathbf{z}_k$$



- Soft interference cancellation using mean of \mathbf{s}_k .
- Assuming Gaussian residual interference and using the covariance of \mathbf{s}_k , compute $\text{LLRs}(\mathbf{s}_k)$.
- Using $\text{LLRs}(\mathbf{s}_k)$, update mean/covariance of \mathbf{s}_k .
- $k \rightarrow \langle k + 1 \rangle_N$.

Iterative Soft ICI Cancellation (BPSK example):



$$\bar{s}_k^{(i)} \triangleq \mathbb{E}\{s_k | \hat{s}_k\} = \tanh(\text{LLR}_k^{(i)} / 2)$$

$$v_k^{(i)} \triangleq \text{var}(s_k | \hat{s}_k) = 1 - (\bar{s}_k^{(i)})^2$$

$$\mathbf{y}_k^{(i)} = \mathbf{x}_k - \mathbf{H}_k \bar{\mathbf{s}}_k^{(i)}$$

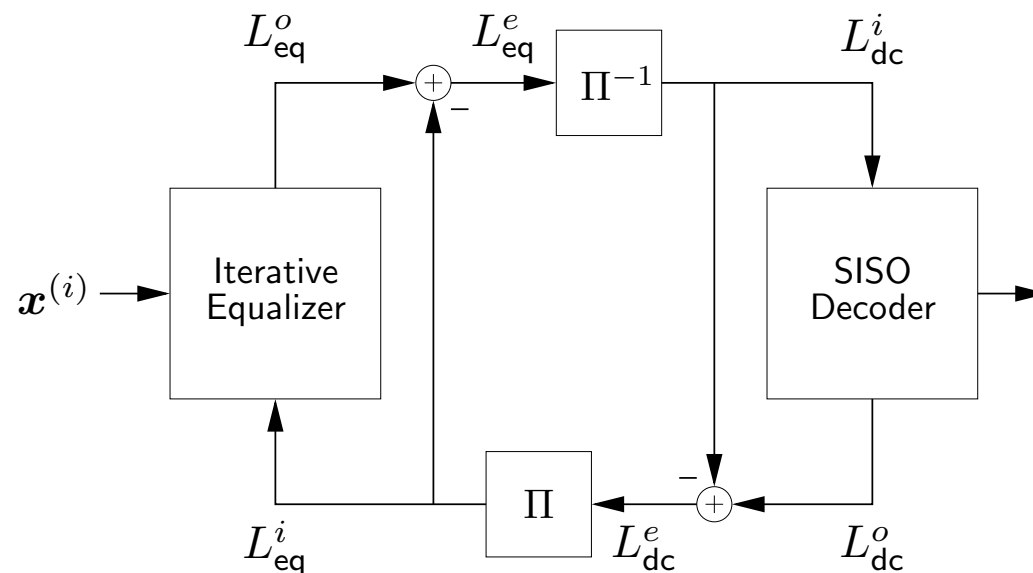
$$g_k^{(i)} = \mathbf{y}_k^{(i)H} (\mathbf{R}_z + \mathbf{H}_k \mathcal{D}(\mathbf{v}_k^{(i)}) \mathbf{H}_k^H)^{-1} \mathbf{h}_k$$

$$\text{LLR}_k^{(i+1)} = \text{LLR}_k^{(i)} + 2 \text{Re}(g_k^{(i)})$$

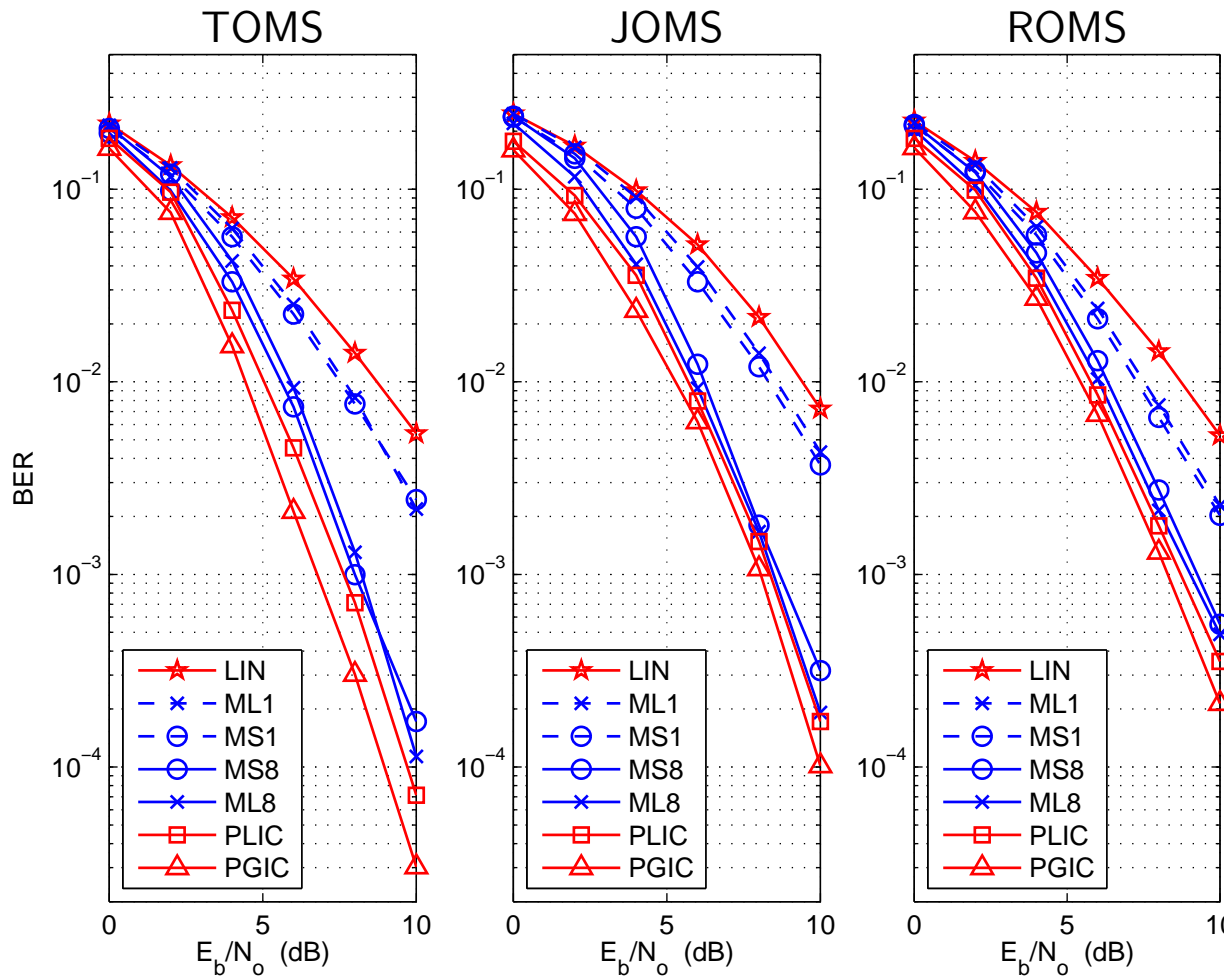
Complexity: $M \times \mathcal{O}(D^2)$ per BPSK symbol.
iters *mtx inv*

Turbo Equalization:

Soft bit information (i.e., LLRs) can be exchanged with a soft-input soft-output (SISO) decoder:



Turbo Equalization Performance:



rate- $\frac{1}{2}$ conv code

QPSK

$N = 64$

$D = 2$

$L = 16$

$f_D T_c = 0.003$

for example:

$f_c = 20\text{GHz}$

$\text{BW} = 3\text{MHz}$

$T_h = 5.4\mu\text{s}$

$v = 3 \times 160\text{km/hr}$

3) Non-Coherent Equalization:

- So far we have assumed that the equalizer is provided with channel estimates.

But with long and quickly varying channels, accurate channel estimation requires a high proportion of pilots!

- Instead, one might consider *joint* estimation of channel and symbols.

Actually, we are not interested in explicitly estimating the channel, but rather doing *non-coherent equalization*: inferring transmitted bits using knowledge of channel statistics but not channel state.

For this it helps to re-parameterize the system model. . .

Basis-Expansion Model:

From the pulse-shaped FDM model:

$$\begin{aligned} \mathbf{x}(n) &= \mathbf{H}(n)\mathbf{s}(n) + \mathbf{z}(n) & \mathbf{H}(n) \text{ is banded with band radius } D \\ &= \mathbf{S}(n)\mathbf{h}(n) + \mathbf{z}(n) & \mathbf{h}(n) \in \mathbb{C}^{(2D+1)N} \text{ ICI coefs} \end{aligned}$$

we can use a basis-expansion model (BEM) for the ICI coefs:

$$\begin{aligned} \mathbf{h}(n) &= \mathbf{B}\boldsymbol{\theta}(n) & \boldsymbol{\theta}(n) \in \mathbb{C}^{(2D+1)L} \text{ delay/Doppler coefs} \\ \mathbf{B} &= \begin{pmatrix} \mathbf{F}_L & & \\ & \ddots & \\ & & \mathbf{F}_L \end{pmatrix} & \mathbf{F}_L \in \mathbb{C}^{N \times L} \text{ truncated DFT matrix} \end{aligned}$$

to rewrite the observation as

$$\mathbf{x}(n) = \mathbf{S}(n)\mathbf{B}\boldsymbol{\theta}(n) + \mathbf{z}(n).$$

Note: if we knew the locations of K active *sparse* taps, we would only include those columns of the DFT matrix, giving $\boldsymbol{\theta}(n) \in \mathbb{C}^{(2D+1)K}$.

Non-coherent MLSD:

Treating the delay/Doppler coeffs $\boldsymbol{\theta}$ as nuisance parameters,

$$\begin{aligned}\hat{\mathbf{s}}_{\text{ML}} &= \arg \max_{\mathbf{s}} p(\mathbf{x}|\mathbf{s}) \\ &= \arg \max_{\mathbf{s}} \int_{\boldsymbol{\theta}} p(\mathbf{x}|\mathbf{s}, \boldsymbol{\theta}) p(\boldsymbol{\theta}) d\boldsymbol{\theta}\end{aligned}$$

Assuming $\boldsymbol{\theta} \sim \mathcal{CN}(\mathbf{0}, \mathbf{R}_{\theta})$,

$$\begin{aligned}\hat{\mathbf{s}}_{\text{ML}} &= \arg \max_{\mathbf{s}} \left\{ \mathbf{x}^H \mathbf{S} \mathbf{B} \boldsymbol{\Sigma}_{\mathbf{s}}^{-1} \mathbf{B}^H \mathbf{S}^H \mathbf{x} - \sigma^2 \log |\boldsymbol{\Sigma}_{\mathbf{s}}| \right\} \\ \boldsymbol{\Sigma}_{\mathbf{s}} &\triangleq \mathbf{B}^H \mathbf{S}^H \mathbf{S} \mathbf{B} + \sigma^2 \mathbf{R}_{\theta}^{-1}\end{aligned}$$

Since $\hat{\boldsymbol{\theta}}_{\text{MMSE}|\mathbf{s}} = \boldsymbol{\Sigma}_{\mathbf{s}}^{-1} \mathbf{B}^H \mathbf{S}^H \mathbf{x}$, we can rewrite

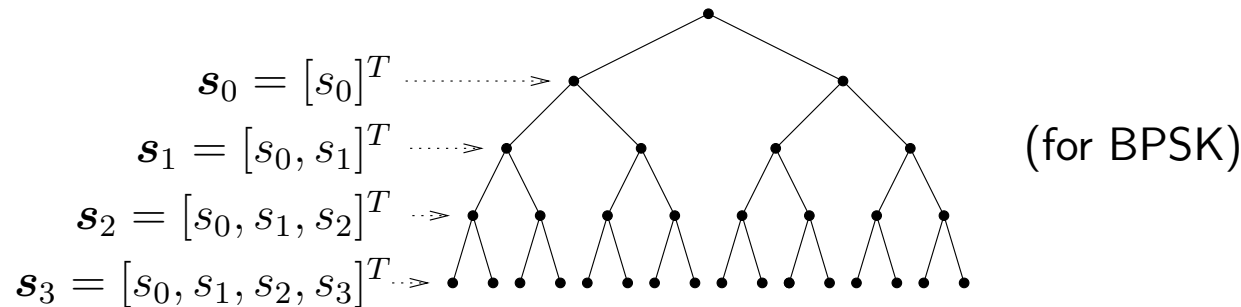
$$\hat{\mathbf{s}}_{\text{ML}} = \arg \max_{\mathbf{s}} \left\{ \|\mathbf{x} - \mathbf{S} \mathbf{B} \hat{\boldsymbol{\theta}}_{\text{MMSE}|\mathbf{s}}\|^2 - \sigma^2 \log |\boldsymbol{\Sigma}_{\mathbf{s}}| \right\}$$

But how do we avoid an exhaustive search over \mathbf{s} ?

Fast Tree Search:

By turning off the first and last D subcarriers, \mathbf{H} becomes upper-triangular, facilitating the use of **tree-search**.

$$\mathbf{x} = \mathbf{H} \mathbf{s} + \mathbf{w}$$



The important thing here is that the *partial* ML metric

$$\mu_{\text{ML}}(\mathbf{s}_k) = \|\mathbf{x}_k - \mathbf{S}_k \mathbf{B}_k \hat{\boldsymbol{\theta}}_{\text{MMSE}|\mathbf{s}_k}\|^2 - \sigma^2 \log |\boldsymbol{\Sigma}_k|$$

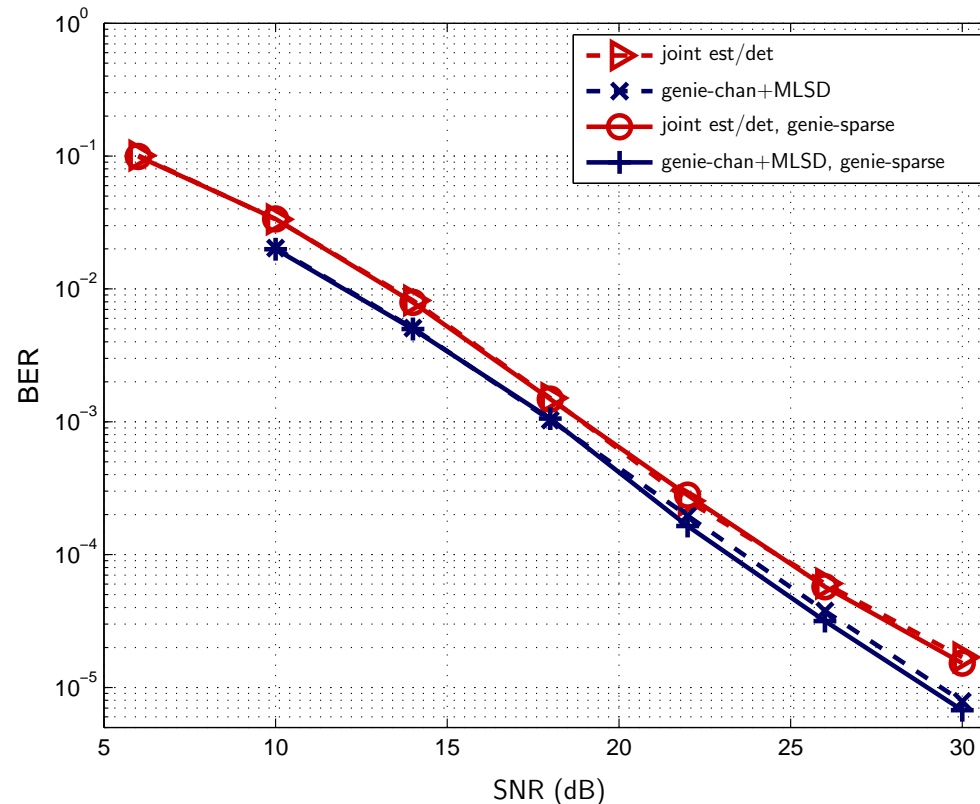
can be computed *recursively*. Thus, total search complexity via the M -algorithm is only

$$2M|\mathcal{S}|(2D + 1)^2 L^2 \text{ mults per QAM-symbol!}$$

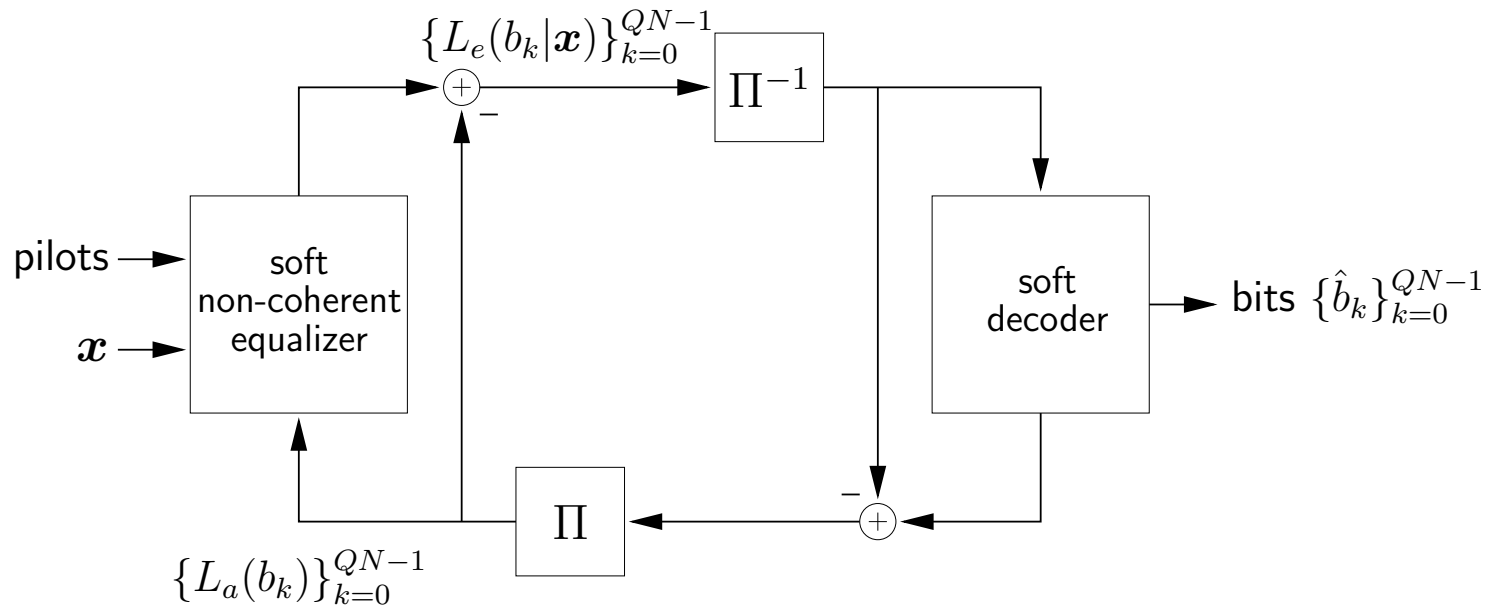
Complexity Reduction via Pilots:

- With non-coherent decoding, we require only a *single* pilot subcarrier.
- But, with more pilots, the initial channel estimate $\hat{\theta}_{\text{MMSE}}$ improves, allowing more aggressive branch pruning in the tree search.

Example: M-algorithm
(BPSK, 25% pilots,
 $M=8$) compared to
coherent MLSD with
genie-aided $\hat{\theta}_{\text{MMSE}}$:



Non-coherent Turbo Equalization:



$$L_e(b_k|\mathbf{x}) = \ln \frac{\sum_{\mathbf{s}: b_k=1} \exp \mu_{\text{MAP}}(\mathbf{s})}{\sum_{\mathbf{s}: b_k=0} \exp \mu_{\text{MAP}}(\mathbf{s})} - L_a(b_k) \quad \text{"extrinsic LLR"}$$

$$\mu_{\text{MAP}}(\mathbf{s}) = \ln p(\mathbf{x}|\mathbf{s}) + \sum_{k: b_k=1} L_a(b_k) \quad \text{"MAP metric"}$$

Need $\mathcal{O}(2^{QN})$ evaluations of $\mu(\mathbf{s}) \rightsquigarrow$ *Computationally infeasible!*

Simplified LLR Evaluation:

The “max-log” approximation:

$$L_e(b_k|\mathbf{x}) \approx \max_{\mathbf{s} \in \mathcal{L} \cap \{\mathbf{s}: b_k=1\}} \mu_{\text{MAP}}(\mathbf{s}) - \max_{\mathbf{s} \in \mathcal{L} \cap \{\mathbf{s}: b_k=0\}} \mu_{\text{MAP}}(\mathbf{s}) - L_a(b_k)$$

\mathcal{L} : set containing the M most probable \mathbf{s} ,

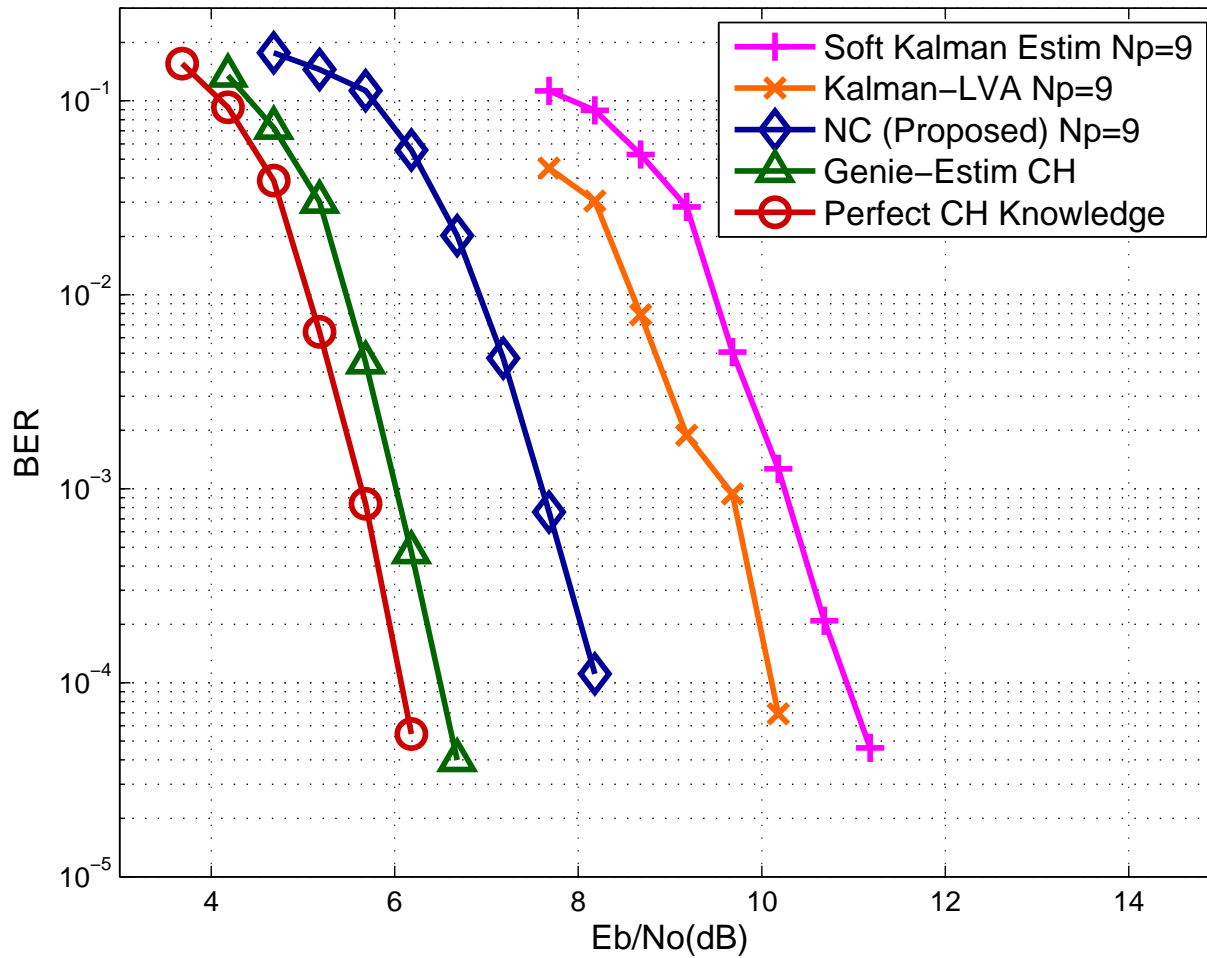
requires only a few evaluations of $\mu_{\text{MAP}}(\mathbf{s})$.

To find \mathcal{L} , the set of most probable \mathbf{s} , and the MAP metrics $\{\mu_{\text{MAP}}(\mathbf{s})\}_{\mathbf{s} \in \mathcal{L}}$, we use a *tree search*, as in the uncoded case.

Here again, there exists a fast metric update such that the total search complexity, with the M-algorithm, is only

$$2M|\mathcal{S}|(2D+1)^2 L^2 \text{ mults per QAM-symbol!}$$

Non-coherent Turbo Performance:



rate- $\frac{1}{2}$ LDPC

QPSK

$N = 64$

$D = 2$

$L = 16$

$K = 3$

$f_D T_c = 0.003$

Related Work:

- Channel estimation techniques (for coherent equalization).
- Single-carrier frequency-domain equalization.
- Pilot pattern designs:
 - MMSE optimal (under CE-BEM assumption).
 - Achievable-rate optimal (under CE-BEM assumption).
- Theoretical analysis of pulse-shaped multicarrier modulation:
 - Achievable-rate characterized.
- Analysis of doubly selective channel:
 - Capacity characterized (under CE-BEM assumption).

(See http://www.ece.osu.edu/~schniter/pubs_by_topic.html)

Conclusions:

Single Carrier:

- $\mathcal{O}(L) \frac{\text{mults}}{\text{QAM symbol}}$ equalization of delay-spread channels.
- Challenging to track quickly time-varying channels.

Orthogonal FDM:

- $\mathcal{O}(\log_2 L) \frac{\text{mults}}{\text{QAM symbol}}$ equalization of delay-spread channels.
- Loss in spectral efficiency due to guard interval.
- Sensitive to Doppler spread.
- Slow spectral roll-off \Rightarrow high adjacent-band interference.

Non-Orthogonal FDM:

- No need for a guard interval; high spectral efficiency.
- Large simultaneous delay & Doppler spreads \Rightarrow no IBI and short ICI.
- Fast spectral roll-off \Rightarrow low adjacent-band interference.

Equalization/Decoding of Short ICI Span:

- *Uncoded Coherent:*

Tree search gives ML-like performance with DFE-like complexity.

- *Coded Coherent:*

Iterative soft ICI cancellation in turbo configuration performs close to perfect-interference-cancellation bound.

- *Uncoded Non-Coherent:*

Tree-search with fast metric update gives ML-like performance with $\mathcal{O}(D^2 L^2)$ complexity.

- *Coded Non-Coherent:*

Tree-search with fast metric update performs close to genie-aided bound with $\mathcal{O}(D^2 L^2)$ complexity, or $\mathcal{O}(D^2 K^2)$ if sparseness leveraged.

Thanks for listening!